DOI 10.1007/s10812-015-0028-9
Journal of Applied Spectroscopy, Vol. 81, No. 6, January, 2015 (Russian Original Vol. 81, No. 6, November–December, 2014)

PHASE EQUILIBRIA AND IONIC SOLVATION IN THE LITHIUM TETRAFLUOROBORATE–DIMETHYLSULFOXIDE SYSTEM

M. M. Gafurov,[a*] S. A. Kirillov,[b,c] M. I. Gorobets,[b] K. Sh. Rabadanov,[a] M. B. Ataev,[a] D. O. Tretyakov,[b] and K. M. Aydemirov[d]

UDC 539.196

The phase diagram and electrical conductivity isotherms for the lithium tetrafluoroborate ($LiBF_4$)–dimethylsulfoxide (DMSO) system and Raman spectra of DMSO and the $LiBF_4$–DMSO solution were studied. Spectroscopic signatures of a H-bond between DMSO and BF_4^- ions were found. The bonds of Li^+ ions to the solvent were stronger than the bonds in DMSO dimers because formation of the solvate destroyed dimeric DMSO molecules. The τ_ω values for DMSO molecules in the Li^+-ion solvate shell of the $LiBF_4$–DMSO system were similar to those for associated solvent molecules.

Keywords: *DMSO, $LiBF_4$, Raman spectra, phase diagram, vibrational dephasing.*

Introduction. Solvation is a complicated phenomenon that accompanies the dissolution of both electrolytes and non-electrolytes [1, 2]. It is described by a combination of energetic and structural changes in the dissolved compound–solvent system and forms a solution of a definite composition. In order to understand if a lithium salt–solvent system satisfies the criteria for battery applications, its phase diagram and concentration dependence of the conductivity are of utmost significance. Vibrational spectroscopy plays an important role among methods for studying equilibria in non-aqueous solvents. Thus, the use of spectroscopic methods can with varying degrees of certainty characterize the solvation of cations and anions, identify ion pairs separated by solvent and more complicated aggregates, and estimate the equilibrium between the various particles in the system [3, 4].

The structure and properties of $LiBF_4$ in aprotic solvents have become interesting in the last decade because of its use as a salt for lithium batteries. We used DMSO [$(CH_3)_2SO$] as the solvent. Equilibria in lithium-salt solutions have been characterized rather well by spectroscopic methods [5, 6]. Spectra in the region of SO stretching vibrations [$\nu_7(A')$, ~1050 cm^{-1}] [7] led to the conclusion that individual unassociated DMSO molecules, cyclic dimers, and chain-like associates were present [8, 9]. The presence of the last was disputed [10]. Furthermore, the ν_7 vibration is known to be subject to a so-called noncoincidence effect and was split into several components in the pure liquid and concentrated solutions [11–13]. Therefore, spectra in the region ~1050 cm^{-1} were difficult to interpret unambiguously. Nevertheless, association constants of DMSO were determined only a few times [14–17]. It was hypothesized that the anions were solvated through H-bonds between DMSO methyls and F atoms in the anion. However, issues regarding the composition of ionic associates in DMSO and other solvents were treated differently [5, 6, 18]. We investigated previously electrolytes for lithium-ion current sources based on dimethylsulfone [19–21]. Because DMSO and dimethylsulfone are close analogs, it seemed interesting to compare the properties of solutions of lithium salts in these solvents.

Experimental. DMSO (Aldrich, ≥98%) was stored over molecular sieves and vacuum distilled. The completeness of the purification was monitored using the melting and boiling points. Anhydrous $LiBF_4$ (Aldrich, ≥98%) was dried in vacuo (vacuum pump) at 150°C for at least 24 h. All samples were prepared in a dry glove box. Phase diagrams of the systems were obtained using differential thermal analysis on a laboratory instrument. The sample mass was ~2.5 g. Electrical conductivity

*To whom correspondence should be addressed.

[a]Analytical Center for Collective Use, Dagestan Scientific Center, Russian Academy of Sciences, 45 M. Gadzhiev Str., Makhachkala, 367025, Russia; e-mail: malik52@mail.ru, rksh83@mail.ru; [b]Inter-Agency Department of Electrochemical Energy Systems, National Academy of Sciences of Ukraine, Kiev; [c]Institute of Sorption and Endoecological Problems, National Academy of Sciences of Ukraine, Kiev; [d]Dagestan State University, Makhachkala, Russia. Translated from Zhurnal Prikladnoi Spektroskopii, Vol. 81, No. 6, pp. 824–830, November–December, 2014. Original article submitted April 9, 2014.

was measured in cells with plane-parallel platinum electrodes using an Instek LCR-821 LCR-meter. Raman spectra were excited using laser radiation (λ = 532 nm) and were recorded using a Senterra confocal laser microscope (Bruker, Germany) in a specially constructed heated attachment with 50 × 100 μm slits and 3–5 cm^{-1} resolution. At least 20 scans with integration time 20 s were accumulated.

Isotropic and anisotropic Raman spectra $I_{iso}(\nu)$ and $I_{aniso}(\nu)$ that were found from spectra recorded in two different scattering geometries VV and VH, where the first and second indices denote the polarization of the incident and scattered light (V, vertical; H, horizontal), were used for the analysis:

$$I_{iso}(\nu) = I_{VV}(\nu) - (4/3)I_{VH}(\nu) , \quad I_{aniso}(\nu) = I_{VH}(\nu) . \tag{1}$$

Information on molecular dynamics in liquids that were obtained by analyzing time-correlated functions (TCF) $G(t)$ was invoked to discern the liquid structures and the cation solvation in them. The TCF were calculated by Fourier transformation of isotropic Raman spectra $I(\nu)$ [22–24]:

$$G(t) = \int_{-\infty}^{+\infty} I(\nu) \exp(2\pi ic\nu t) d\nu , \tag{2}$$

where c is the speed of light. Vibrational dephasing was considered to be the main reason for broadening of the isotropic Raman lines. Interaction of a particle and its environment with vibrational dephasing (excitation) led to time-dependent changes (modulation) of the vibrational frequency $\Delta\omega = f(t)$ and a breakdown of the vibration phase. If the vibrational frequency changes exponentially with time, $G_\omega(t) = \exp(-t/\tau_\omega)$, where τ_ω is the modulation time, then the TCF of vibrational dephasing obeys the Kubo equation [25]:

$$-\ln G(t)/M_2 \quad = \exp(-t/\tau_\omega) - 1 + t/\tau_\omega , \tag{3}$$

where $M_2 = \int \nu^2 I(\nu) d\nu / \int I(\nu) d\nu$ is the second moment of the vibrational spectrum (excitation dispersion). The TCF and the spectrum change as a function of excitation time. For $\tau_\omega \to 0$ (dynamic particle environment, weak excitation, nonspecific interactions), the dephasing TCF are exponential and the spectra are Lorentzian; for $\tau_\omega \to \infty$ (specific and non-specific strong excitations, rigid quasi-lattice of molecules and environment), the dephasing TCF and spectra become Gaussian. The dephasing time τ_V acts as another parameter. It is defined as the integral of $G(t)$:

$$\tau_V = \int G(t) dt. \tag{4}$$

The literature method [26, 27] was used to separate complicated Raman envelopes into components and to calculate the TCF. A model TCF was used in it:

$$G_\nu(t) = \exp\{-[(t^2 + \tau_1^2)^{1/2} - \tau_1]/\tau_2\} , \tag{5}$$

where τ_1 and τ_2 were certain times. Fourier transformation of this TCF could be performed analytically to provide an expression for the line envelope:

$$I(\nu) = 2nc \exp(\tau_1/\tau_2)(\tau_1^2/\tau_2) K_1(x)/x , \tag{6}$$

where $x = \tau_1[4\pi^2 c^2(\nu - \nu_0)^2 + 1/\tau_2^2]^{1/2}$; ν_0 is the wavenumber of the line maximum; $n = 2$ for $\nu_0 = 0$ and $n = 1$ for $\nu_0 \neq 0$; and $K_1(x)$ is a modified second-order Bessel function. This method is widely used to process spectroscopic data [28], especially to separate overlapping lines. The experimental spectrum consisting of i lines was modeled by a set of i functions [Eq. (6)]. The quantities τ_{1i} and τ_{2i} were found. Then, M_2 was found for each i-th line. The TCF were constructed using Eq. (5). The quantities τ_ω at which Eqs. (3) and (5) coincided were determined. As before [29, 30], the intensities of the resulting envelope components were considered to be proportional to concentrations without introducing corrections for possible differences in the scattering abilities of the corresponding particles.

Herein we report data for equilibria between particles in the $LiBF_4$–DMSO system that were obtained by investigating phase diagrams, electrical conductivity, and Raman spectra over a broad concentration range up to 0.25 mol fraction of salt, which corresponded to a homogeneous mixture of $LiBF_4 \cdot 4DMSO$ crystal solvate with $LiBF_4$. In contrast with other similar studies, we described all equilibrium without exception, invoking for the analysis data on self-association of DMSO molecules in the liquid [31]. We proved that the solutions contained ions separated by solvent and contact ion pairs and presented for the first time reliable evidence for H-bonds between the anions and DMSO.

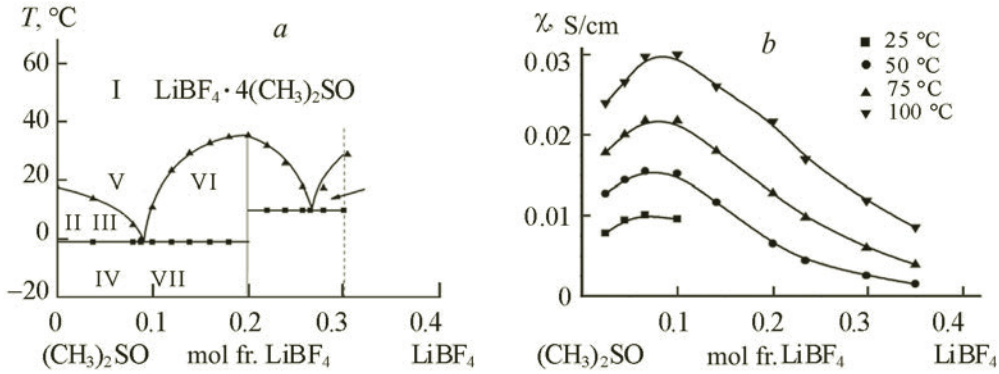

Fig. 1. Phase diagram (a) and electrical conductivity isotherms (b) for the $LiBF_4$–DMSO system.

Results and Discussion. Interaction of $LiBF_4$ and the solvent was rather strong and manifested as the existence of the stable solvate $LiBF_4 \cdot 4DMSO$ (Fig. 1a). Typical isotherms of specific electrical conductivity for the electrolyte solutions reflected the interaction between the dissolved compound and the solvent and exhibited a maximum. The ascending branch of the isotherm was consistent with an increasing number of charge carriers; the descending branch, with the formation of ion pairs and increased viscosity. Electrical conductivity isotherms of $LiBF_4$–DMSO solutions showed distinct conductivity maxima at salt concentrations ~0.1 mol fr. (Fig. 1b). This indicated that the studied systems acted as solutions of strong electrolytes. Therefore, it could be expected that solvated cations and ion pairs would be present at high solution salt concentrations.

We did not analyze DMSO lines complicated by the noncoincidence effect that corresponded to the SO stretching vibration (~1050 cm^{-1}) in order to obtain unambiguous data for the liquid components. We did investigate Raman spectra near the DMSO C–S–C stretching vibration [$\nu_{10}(A')$, ~697 cm^{-1}]. Figure 2 shows that the line in the DMSO Raman spectrum corresponding to the DMSO C–S–C symmetric stretching vibration (ν_{10}) consisted of two components, i.e., a low-frequency one corresponding to vibrations of monomers and a high-frequency one corresponding to vibrations of DMSO dimers. The intensity of the low-frequency component increased with temperature whereas the low-frequency one decreased. This indicated that the associates decomposed. A depolarized line near 700 cm^{-1} corresponded to DMSO C–S–C asymmetric stretching vibration $\nu_{22}(A'')$ [8]. The component at lower frequencies had a practically Lorentzian shape whereas that at higher frequencies was close to Gaussian. In this instance, it was justified to assign the first component to free DMSO molecules; the second, to associated ones. The calculated modulation times showed that τ_ω for associated molecules was two orders of magnitude greater than that for free ones (Table 1).

Figure 3 shows characteristic examples of spectra of $LiBF_4$ in DMSO. Isotropic Raman spectra near the DMSO C–S–C symmetric stretching vibration $\nu_{10}(A') \sim 670$ cm^{-1} were investigated in order to obtain information on cation solvation. A line corresponding to the C–S–C asymmetric stretching vibration $\nu_{22}(A'') \sim 700$ cm^{-1} was situated in the same region. It was more noticeable in the anisotropic spectrum. Anion solvation was judged from isotropic spectra near DMSO C–H symmetric stretching vibration $\nu_3(A') \sim 2910$ cm^{-1}. The anisotropic spectrum had a line corresponding to $\nu_{14}(A'')$ at ~3000 cm^{-1} in this same region. Conclusions about ion-pair formation were made based on spectra of BF_4^- near fully symmetric $\nu_1(A_1)$ at ~760 cm^{-1} [32].

Three lines were distinguishable near the DMSO C–S–C symmetric stretching vibration (Fig. 3a). The line at lowest frequency belonged to DMSO monomers; at intermediate frequency, to DMSO dimers; and at highest frequency, to solvent molecules in the Li^+ solvation sphere. The calculated modulation times indicated that τ_ω for DMSO molecules in the Li^+ solvent shell also had τ_ω values intermediate between those for associated and free molecules. Figure 4 shows the equilibrium concentrations of monomers (c_M), dimers (c_D), and solvated molecules (c_S) as functions of the solution composition (curves 1–3). It can be seen that c_D decreased faster than c_M as the salt concentration increased. Therefore, the formation of the solvates led to the destruction of cyclic DMSO dimers that were formed through dipole–dipole bonds, i.e., the ion–dipole bond of Li^+ and the solvent was stronger than the dipole–dipole bond in the dimers. Available data on equilibria between dimers and monomers in pure DMSO, in particular the enthalpy of self-association (–11.7 ± 0.9 kJ/mol) [22], confirmed convincingly that the enthalpy of formation of the solvates was greater than this value.

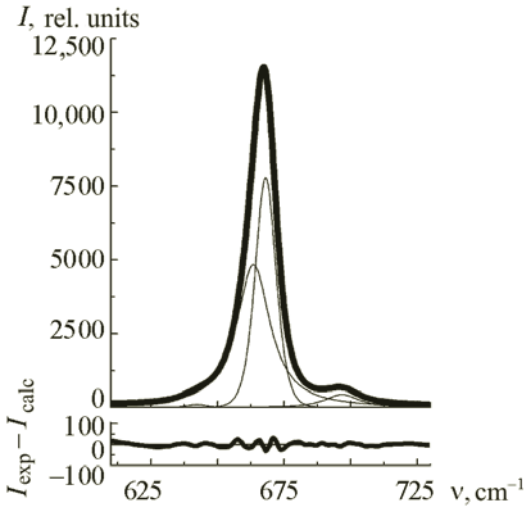

Fig. 2. Isotropic Raman spectrum of DMSO near the symmetric and asymmetric C–S–C stretching vibrations (ν_{10}) at 50°C; thin lines, deconvolution of spectra into components; $I_{exp} - I_{calc}$, differences of experimental and calculated values.

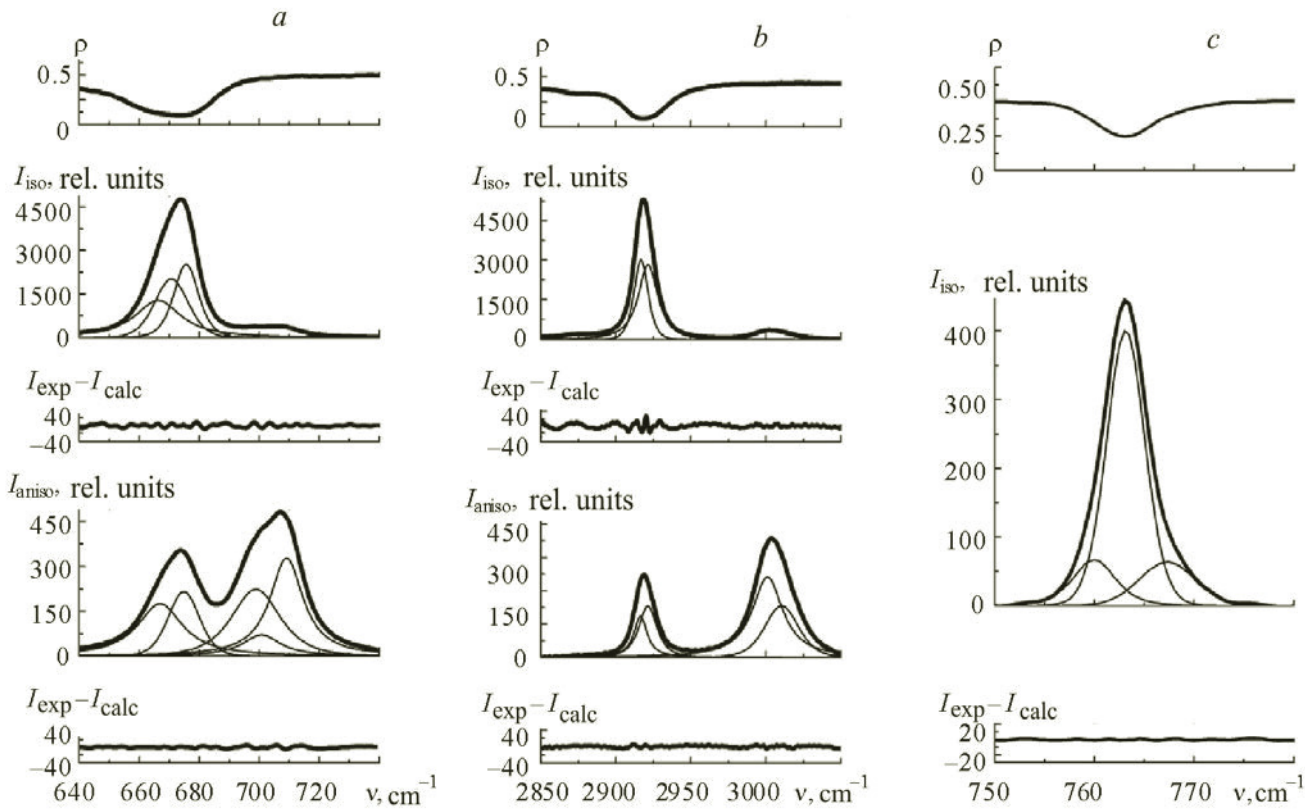

Fig. 3. Raman spectra of $LiBF_4$–DMSO (0.15:0.85) solutions at 50°C; thin lines, deconvolution of spectra into components; $\rho = I_{VH}/I_{VV}$, degree of line depolarization; $I_{exp} - I_{calc}$, differences of experimental and calculated values; DMSO C–S–C stretching vibration region (a); DMSO C–H vibration region (b); fully symmetric BF_4^- vibration region (c).

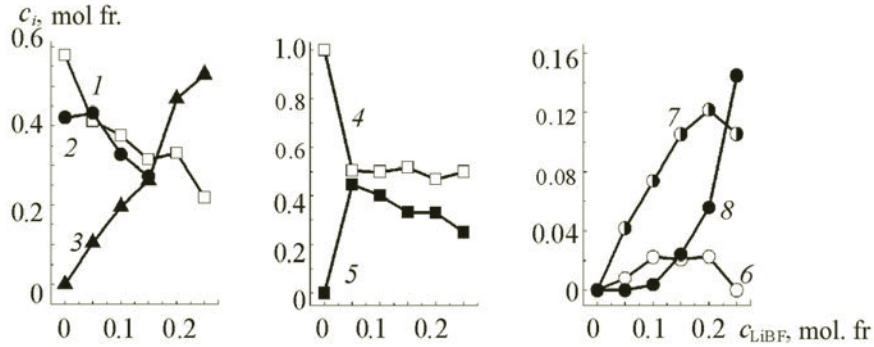

Fig. 4. Concentrations of monomeric (1), dimeric (2), and DMSO molecules in the Li^+ solvation sphere (3); of free solvent molecules (4) and those in the BF_4^- anion solvation sphere (5); of free anions (6); of solvent-separated ion pairs (7); and of contact ion pairs (8) as functions of solution composition.

TABLE 1. Dephasing Parameters of $\nu_{10}(CH_3)_2SO$ Vibrations in $LiBF_4$–$(CH_3)_2SO$

Salt concentration, mol fr.	0	0.05	0.10	0.15	0.20	0.25
Free $(CH_3)_2SO$						
ν, cm^{-1}	663.87	663.51	665.78	665.82	666.49	666.78
τ_V, ps	0.70	0.64	0.68	0.68	0.69	0.64
τ_ω, ps	0.026	0.025	0.024	0.024	0.023	0.018
M_2, ps^{-2}	56.82	63.92	62.47	62.53	64.48	87.89
Associated $(CH_3)_2SO$						
ν, cm^{-1}	668.22	668.39	670.27	671.07	671.90	676.21
τ_V, ps	1.61	1.41	1.20	1.32	1.56	1.24
τ_ω, ps	2.57	2.28	2.36	4.36	5.73	3.78
M_2, ps^{-2}	0.78	1.014	1.34	1.02	0.73	1.18
Li^+–$(CH_3)_2SO$ solvate						
ν, cm^{-1}		675.26	675.64	675.70	675.82	676.27
τ_V, ps		1.07	1.217	1.41	1.33	1.15
τ_ω, ps		0.097	0.118	1.31	1.45	0.83
M_2, ps^{-2}		10.55	7.69	1.21	1.29	2.013

A study of pure liquid DMSO led to the conclusion that its molecules did not tend to form H-bonds. A single line was observed in the region of the C–H symmetric stretching vibration [33]. Deconvolution of the spectra of the ionic solutions into components showed unambiguously that two lines appeared in them in this region (Fig. 3b). The lower frequency line belonged to free DMSO molecules; the higher frequency line, to solvent molecules in the BF_4^- solvation sphere that were bonded to it through H-bonds. Figure 4 (curves 4 and 5) shows the equilibrium concentrations of free and H-bonded DMSO molecules (c_F and c_H) as functions of solution composition. Three lines appeared near the fully symmetric vibration of BF_4^-. The one at lowest frequency belonged to free anions; at intermediate frequency, to ion pairs separated by solvent; at highest frequency, to contact ion pairs (Fig. 3c). Figure 4 (curves 6–8) shows the equilibrium concentrations of these particles (c_A, c_{SSIP}, and c_{CIP}) as functions of solution composition.

The composition of the solution structural units could easily be estimated quantitatively by knowing the dependence of the particle concentrations (c_M, c_D, c_S, c_F, c_H, c_A, c_{SSIP}, and c_{CIP}) on the salt content. This was important for defining the nature of the ion pairs more clearly. It was noted above that the literature is ambiguous about their composition and that the issue of differences between solvent-separated ion pairs, contact ion pairs, and more complicated cation–anion aggregates remains unresolved [5, 6].

The following limitations must be kept in mind when estimating the composition of the structural units. Because neither monomeric nor dimeric molecules in pure DMSO are bonded through H-bonds, it was logical to think that DMSO dimers in ionic solutions also did not participate in H-bonds, i.e., $c_H \notin c_D$. Monomeric DMSO molecules in ionic solutions could be either completely free or involved in H-bonds, i.e., $c_H \subseteq c_M$. Solvent molecules around the cation were firstly the solvate environment itself and secondly, an interlayer between the cation and anion in solvent-separated ion pairs, i.e., $c_{SSIP} \subseteq c_S$. Considering these limitations, it could be concluded that, e.g., solvent-separated ion pairs of composition $DMSO{\cdot}Li^+{\cdot}DMSO{\cdot}BF_4^-{\cdot}3DMSO$ existed in the solution containing 0.10 mol fr. $LiBF_4$. The most concentrated solutions studied by us (0.25 mol fr. $LiBF_4$) contained solvent-separated ion pairs with fewer solvent molecules around the cation and H-bonded anion and had the composition $Li^+{\cdot}DMSO{\cdot}BF_4^-{\cdot}DMSO$. Contact ion pairs $2DMSO{\cdot}Li^+{\cdot}BF_4^-{\cdot}DMSO$ appeared in addition to them.

The correlation of the changes of dephasing parameters and modulation with Li salt–DMSO phase diagrams was especially interesting. The τ_ω values for DMSO molecules in the Li^+ solvate shell were close to those for associated solvent molecules for the $LiBF_4$–DMSO system in which a coherently melting compound (solvate $LiBF_4{\cdot}4DMSO$) was observed.

Conclusions. The $LiBF_4$–DMSO system contained the stable solvate $LiBF_4{\cdot}4DMSO$. The line corresponding to the DMSO C–S–C symmetric stretching vibration in the Raman spectrum consisted of two components, i.e., a low-frequency one corresponding to monomer vibrations and a high-frequency one corresponding to dimer vibrations. Because formation of the solvates destroyed the DMSO dimers, the Li–solvent bond was stronger than the bond in the dimers, i.e., greater than the enthalpy of DMSO self-association. The τ_ω values for DMSO molecules in the Li^+ solvate shell were similar to those for associated solvent molecules in the $LiBF_4$–DMSO system.

Acknowledgments. The work used equipment of the Analytical Center for Collective Use, Dagestan Scientific Center, RAS and was supported financially by the Russian Federation Ministry of Education and Science (SC No. 16.552.11.7092) and the Russian Foundation for Basic Research (Grant No. 13-03-00384_a).

REFERENCES

1. K. P. Mishchenko and G. M. Poltoratskii, *Thermodynamics and Structure of Aqueous and Non-Aqueous Electrolyte Solutions* [in Russian], Khimiya, Leningrad (1976).
2. N. A. Izmailov, *Electrochemistry of Solutions* [in Russian], Khimiya, Moscow (1966).
3. K. Xu, *Chem. Rev.*, **104**, 4304–4418 (2004).
4. D. Martin, A. Weise, and H.-J. Niclas, *Angew. Chem., Int. Ed.*, **6**, 318–334 (1967).
5. I. S. Perelygin, in: *Ionic Solvation*, G. A. Krestov (Ed.), Ellis Horwood, Chichester (1994), pp. 100–207.
6. J. M. Alia, in: *Handbook of Raman Spectroscopy*, I. R. Lewis and H. G. M. Edwards (Eds.), Marcel Dekker, New York (2001), pp. 617–683.
7. M. T. Forel and M. Tranquil, *Spectrochim. Acta, Part A*, **26**, No. 8, 1023–1034 (1970).
8. I. S. Perelygin, A. S. Krauze, and I. G. Itkulov, *Zh. Prikl. Spektrosk.*, **52**, No. 3, 414–419 (1990).
9. I. S. Perelygin, I. G. Itkulov, and A. S. Krauze, *Zh. Fiz. Khim.*, **65**, 410–413 (1991).
10. W. R. Fawcett and A. A. Kloss, *J. Chem. Soc. Faraday Trans.*, **92**, 3333–3337 (1996).
11. G. Fini and P. Mirone, *Spectrochim. Acta, Part A*, **32**, 625–629 (1976).
12. C. Czeslik, Y. J. Kim, and J. Jonas, *J. Chem. Phys.*, **111**, 9739–9742 (1999).
13. M. Paolantoni, M. E. Gallina, and P. Sassi, *J. Chem. Phys.*, **130**, 164501–164509 (2009).
14. Z. Lu, E. Manias, and D. D. Macdonald, *J. Phys. Chem. A*, **113**, 12207–12214 (2009).
15. T. Shikata and N. Sugimoto, *Phys. Chem. Chem. Phys.*, **13**, 16542–16547 (2011).
16. R. H. Figueroa, E. Roig, and H. H. Szmant, *Spectrochim. Acta*, **22**, 587–592 (1966).
17. T. Shikata and N. Sugimoto, *J. Phys. Chem. A*, **116**, 990–999 (2012).
18. X. Xuan, J. Wang, and Y. Zhao, *J. Raman Spectrosc.*, **38**, 865–872 (2007).
19. D. O. Tretyakov, V. D. Prisiazhnyi, M. M. Gafurov, K. Sh. Rabadanov, and S. A. Kirillov, *J. Chem. Eng. Data*, **55**, 1958–1964 (2010).

20. M. M. Gafurov, K. Sh. Rabadanov, V. D. Prisyazhnyi, D. O. Tret′yakov, M. I. Gorobets, S. A. Kirillov, M. B. Ataev, and M. M. Kakagasanov, *Zh. Fiz. Khim.*, **85**, No. 9, 1615–1619 (2011).
21. M. M. Gafurov, K. Sh. Rabadanov, M. B. Ataev, A. R. Aliev, I. R. Akhmedov, M. G. Kakagasanov, and S. P. Kramynin, *Zh. Prikl. Spektrosk.*, **79**, No. 2, 200–205 (2012).
22. W. G. Rothschild, *Dynamics of Molecular Liquids*, Wiley, New York (1984).
23. C. H. Wang, *Spectroscopy of Condensed Media. Dynamics of Molecular Interactions*, Academic, Orlando (1985).
24. D. W. Oxtoby, *Adv. Chem. Phys.*, **40**, 1–48 (1979).
25. R. A. Kubo, *Fluctuations, Relaxation and Resonance in Magnetic Systems*, G. ter Haar (Ed.), Scottish Universities′ Summer School 1961, Oliver and Boyd, Edinburgh (1962), pp. 23–68.
26. S. A. Kirillov, *Chem. Phys. Lett.*, **303**, 37–42 (1999).
27. S. A. Kirillov, *Pure Appl. Chem.*, **76**, 171–181 (2004).
28. S. A. Kirillov, in: *Novel Approaches to the Structure and Dynamics of Liquids: Experiments, Theories and Simulations*, NATO ASI Series, J. Samois and V. Durov (Eds.), Kluwer, Dordrecht (2004), pp. 193–227.
29. G. M. Photiadis and G. N. Papatheodorou, *J. Chem. Soc. Dalton Trans.*, **6**, 981–990 (1998).
30. S. A. Kirillov, A. Morresi, and M. Paolantoni, *J. Phys. Org. Chem.*, **20**, 568–573 (2007).
31. S. A. Kirillov, M. I. Gorobets, M. M. Gafurov, K. Sh. Rabadanov, and M. B. Ataev, *Zh. Fiz. Khim.*, **88**, No. 1, 140–142 (2014).
32. H. Siebert, *Anwendungen der Schwingungsspectroscopie in der anorganischen Chemie*, Springer, Berlin (1966).
33. S. A. Kirillov, M. I. Gorobets, M. M. Gafurov, M. B. Ataev, and K. Sh. Rabadanov, *J. Phys. Chem. B*, **117**, 9439–9448 (2013).